NUMERICAL INVESTIGATION OF UNSTEADY FREE CONVECTIVE MICROPOLAR FLUID FLOW BETWEEN PARALLEL PLATE

FERDOUSE, J.[1] – ISLAM, M. M.[1] – FOISAL, A. A.[1] – ALAM, M. M.[2*]

[1] *Department of Mathematics, University of Barishal, Barishal, Bangladesh.*

[2] *Mathematics Discipline, Khulna University, Khulna, Bangladesh.*

**Corresponding author*
e-mail: alam_mahmud2000[at]yahoo.com

(Received 10th February 2024; revised 03rd May 2024; accepted 10th May 2024)

Abstract. An extensive computational analysis was conducted to examine the dynamics of unsteady natural convective flow involving a micro-polar fluid confined between two parallel horizontal plates with both plates being stationary. Through employing conventional transformation, the governing equations, initially in the form of partial differential equations, have been converted into dimensionless equations which have been subsequently solved using the finite difference technique. The numerical solutions were obtained using both MATLAB R2015 and Studio Developer FORTRAN 6.6a. The case is considered to be related to the disappearance of the anti-symmetry component of the stress tensor, which indicates a subtle concentration. To comprehensively understand the impact of physical parameters, rigorous analysis was performed on stability and convergence criteria. Employing an appropriate mesh space, the impact of various parameters on key factors like velocity, angular velocity and temperature local shear stress, couple stress and the Nusselt number has been investigated. The outcomes of this analysis have been visualized through graphical representations. The dimensionless time is obtained by the time-sensitivity test, while the mesh sensitivity tests as well as the validation test have been conducted and presented. Finally, the attained outcomes were compared with the published findings, which were shown graphically for a comprehensive evaluation.
Keywords: *micropolar fluid, heat transfer, horizontal walls, finite difference technique, suction, stability analysis*

Introduction

A dynamic medium characterised by its properties and actions are intricately connected to the motion of individual material particles within each volume unit is referred to as a simple micro-fluid. These micro-fluids show the attribute of viscosity and possess local inertia. Micropolar fluids are consisting of microstructure which considers a number of several flow situations such as the flow of low concentration suspensions. Micropolar fluids have many great applications in engineering and industrial. This micropolar fluid model has proven to valuable in exploring the characteristics of inherent anisotropy present in complex fluid like liquid crystal with dumbbell-shaped molecules, unconventional lubricants, the movement of colloidal suspensions, biological blood and turbulent shear flows. Eringen (1964) formulated a simple microfluid that introduced the notion of inertial spin, body moments, micro stress averages and stress moments concept absents in classical fluid theories. Eringen (1966) delved into the theory of micropolar fluids, addressing a category of fluid that manifest micro-rotational influences and micro-rotational inertia. This theory also described the micropolar fluids are capable of sustaining couple stress and body couples only. Furthermore, Eringen (1972) presented the theory of thermomicrofluids. Galdi and

Rionero (1977) conducted an investigation on the solution of uniqueness and existence for the equations that govern micropolar flow. Takhar and Soundalgekar (1985) investigated the dynamics of heat transfer past a porosity wall of the micropolar fluid. Mujaković (1998) has conducted a study of unidirectional flow in a compressible micropolar viscous fluid, including the development of a local existence theorem.

Bhargava et al. (2003) formulated a numerical approach for solving the problem of free convection in magnetohydrodynamics micropolar fluid flow constrained between two vertical parallel porous plates. Examining transient convective flow, Rahman and Sattar (2007) analysed the behavior of micropolar fluids as it passed a continually moving vertical porous plate under the influence of radiation. Lok et al. (2010) proposed the stagnation point boundary layer flow with slip within a micropolar fluid. Achieving solution stability for the Cauchy problem for a one-dimensional viscous compressible micropolar fluid has been studied by Mujaković (2010). Revi et al. (2013) explored the transient nature of natural convective flow within a micropolar fluid confined between two perpendicular plates. Mohanty et al. (2015) conducted a numerical investigation to examine the impact of a micropolar fluid flowing upon a stretching sheet positioned within a porous medium. Turkyilmazoglu (2016) developed a model to study the micropolar fluid flow due to a permeable extending sheet, taking heat conduction. Hayat et al. (2017) examined homogeneous-heterogeneous reactions within the context of magneto-hydrodynamics motion of micro-polar fluid over a curved stretching surface. The impact of thermal and mass transfer on time varying natural convective MHD motion of a micro-polar fluid enclosed by two perpendicular walls was investigated by Patel (2021). Hence the main objective of this research is to explore the characteristics of unsteady free convective micro-polar fluid motion through a parallel plate. The introduced model has been transformed into a set of non- similar coupled partial differential equations through standard transformations. The dimensionless time is obtained by the time-sensitivity analysis. Also, the mesh sensitivity test as well as the validation test has been shown. Finally, some significant findings of this investigation have been computed and displayed.

Mathematical model of the flow

The physical configurations of the investigated scenario have been presented in *Figure 1* where an unsteady and incompressible micropolar fluid flow confined between two horizontal plates situated at distinct planes $y=\pm L$. The lower and upper of both plates are stationary. The upper plate is maintained at a set temperature T_h and lower plate is retains a constant temperature T_c. The flow variables will depend only on the coordinate, y and time, t. Given that the plates are of infinite long, all derivatives concerning x are presumed to be zero, $\partial u/\partial x = 0$, and the continuity $(\partial u/\partial x)+(\partial v/\partial y) = 0$, give that $\partial v/\partial y = 0$. It is to be mentioned that v_0 is the suction velocity.

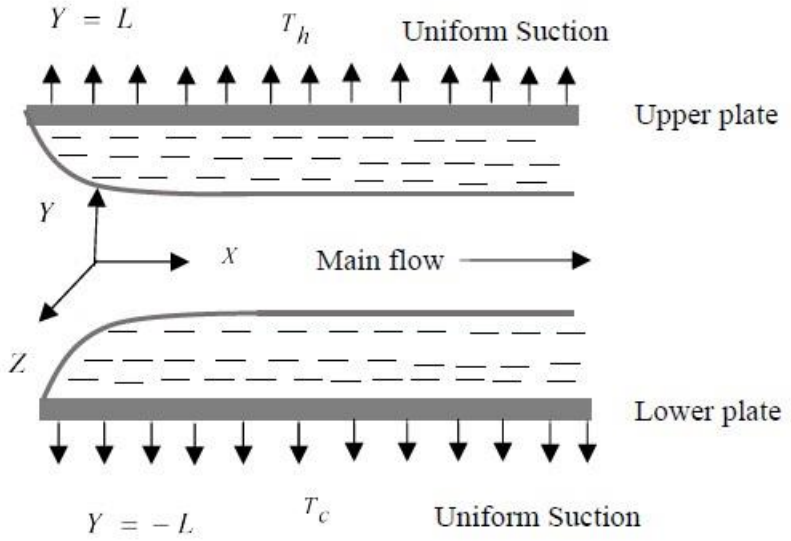

Figure 1. *Illustration of physica setup and co-ordinate system.*

According to the specified assumptions, the equation governing the dynamics of time variant natural convective flow of a micro-polar fluid enclosed by two fixed horizontal parallel plates is directed by the subsequent nonlinear set of combined partial differential equations. These equations, subject to boundary-layer approximations can be expressed as follows:

Continuity equation:

$$v=\text{constant}=-v_0 \qquad \text{Eq. (1)}$$

Momentum equation:

$$\frac{\partial u}{\partial t}-v_o\frac{\partial u}{\partial y}=\left(\frac{(\mu+\lambda)}{\rho}\right)\left(\frac{\partial^2 u}{\partial y^2}\right)+\lambda\frac{\partial \omega}{\partial y}+\rho g\beta\left(T'-T_m{}'\right) \qquad \text{Eq. (2)}$$

Angular momentum equation:

$$\frac{\partial \omega}{\partial t}-v_o\frac{\partial \omega}{\partial y}=\left(\frac{(\mu+.5\lambda)}{\rho}\right)\left(\frac{\partial^2 \omega}{\partial y^2}\right)-\frac{\lambda}{\rho j}\left(2\omega+\frac{\partial u}{\partial y}\right) \qquad \text{Eq. (3)}$$

Energy equation:

$$\frac{\partial T'}{\partial t}-v_o\frac{\partial T'}{\partial y}=\alpha\left(\frac{\partial^2 T'}{\partial^2 y}\right)+\frac{1}{\rho c_p}(\mu+\lambda)\left[\left(\frac{\partial u}{\partial y}\right)^2\right] \qquad \text{Eq. (4)}$$

Where; the components of velocity along *x* and *y* axes are *u* and *v*, *w* represents the component of the micro-rotation vector perpendicular to the *x*, *y* plane, T_m denotes temperature of the fluid, g stands for the magnitude of the gravitational acceleration, β is

thermal expansion coefficient, λ is the vortex viscosity, ν is the kinematic viscosity, j is the micro-inertia density. The corresponding boundary conditions are expressed below:

$$t \le 0, \quad u = 0,\ \omega = 0, T' = T'_m \qquad y \le 0 \le L \qquad \text{Eq. (5)}$$

$$t > 0, \quad u = 0,\ \omega = -n\frac{\partial u}{\partial y},\ T' = T'_h \qquad \text{at } y = L$$

$$u = 0, \quad \omega = 0, \quad T' = T'_c \qquad \text{at } y = -L \qquad \text{Eq. (6)}$$

The spin gradient viscosity is denoted by $\gamma = \left(\mu + \frac{\lambda}{2}\right)j$. n be the surface condition parameter and varying between 0 to 1. Notably, when $n = 0$, it implies a scenario of weak concentration where micro rotation near the wall is absent. On the other hand, for n=0.5 indicates the elimination of the anti-symmetric segment of the stress tensor and signifying stronger concentrations. The scenario $n = 1$ is often employed to model turbulent boundary layer flows. To derive the dimensionless governing equations and boundary conditions, the following non-dimensionl parameters are utilized:

$$X = \frac{x\nu^2}{\beta g L^4\left(T'_h - T'_m\right)}, Y = \frac{y}{L}, U = \frac{u\nu}{\beta g L^2\left(T'_h - T'_m\right)}, T = \frac{\left(T' - T'_m\right)}{\left(T'_h - T'_m\right)}, \tau = \frac{\nu t}{L^2}, \Omega = \frac{\omega\nu}{\beta g L\left(T'_h - T'_m\right)} \qquad \text{Eq. (7)}$$

The gained dimensionless governing equations are written as follows:

$$\frac{\partial U}{\partial \tau} - S\frac{\partial U}{\partial Y} = \left(1 + \Delta\right)\left(\frac{\partial^2 U}{\partial Y^2}\right) + \Delta\frac{\partial \Omega}{\partial Y} + T \qquad \text{Eq. (8)}$$

$$\frac{\partial \Omega}{\partial \tau} - S\frac{\partial \Omega}{\partial Y} = \left(1 + .5\Delta\right)\frac{\partial^2 \Omega}{\partial Y^2} - \Delta\Theta\left(2\Omega + \frac{\partial U}{\partial Y}\right) \qquad \text{Eq. (9)}$$

$$\frac{\partial T}{\partial \tau} - S\frac{\partial T}{\partial Y} = \frac{1}{P_r}\frac{\partial^2 T}{\partial \tau^2} + \left(1 + \Delta\right)\left(\frac{\partial U}{\partial Y}\right)^2 E_c \qquad \text{Eq. (10)}$$

The noted equations are introduced various relevant parameters which have great effects on the flow pattern. The non-dimensional parameters are demonstrated below:

$$P_r = \frac{\nu}{\alpha}(\text{Prandtl number}),\ \Delta = \frac{\lambda}{\mu}(\text{microrotation number}), E_c = \frac{\beta g L^4\left(T'_h - T'_m\right)}{C_p \nu^2}(\text{Eckert number})$$

$$\varsigma = \frac{T'_c - T'_m}{T'_h - T'_m}(\text{Ratio parameter}), \Theta = \frac{L^2}{j}\ (\text{Material parameter}), S = \frac{v_0 L}{\nu}. \qquad \text{Eq. (11)}$$

Hence the criteria for the non-dimensionl starting as well as boundary criteria are defined as:

$$\begin{aligned}
&\tau \le 0,\ U = \Omega = 0,\ T = 0,\ 0 \le Y \le 1 \\
&\tau > 0,\ U = 0,\ \Omega = -N\frac{\partial U}{\partial Y},\ T = 1 \quad \text{at } Y = 1 \\
&U = \Omega = 0,\quad T = \varsigma \qquad \text{at } Y = -1
\end{aligned} \qquad \text{Eq. (12)}$$

Solution strategy

The numerical solution was obtained employing the explicit finite difference technique for solving the non-dimensional differential Eq. (5) to Eq. (7) according to specified boundary conditions. The area inside the boundary zone is parted into a mesh or grid composed of lines which is parallel to the X and Y axes where the X-axis aligns with the plate and the Y-axis is perpendicular to the plate. The height of the plate reached a maximum value $X_{\max} = (5)$ indicated X changes from 0 to 5.The boundary condition strongly displays that the upper plate is located at Y=1 and the lower plate is situated at Y=-1 and consider corresponding $Y_{\max} = (2)$ indicates Y ranging from 0 to 2. The parameters ΔX and ΔY represents the constant mesh spacing along X and Y directions respectively are displayed in *Figure 2* with $\Delta X = 0.125(0 \le x \le 5)$, $\Delta Y = 0.05(0 \le y \le 2)$ considering the minimal time step $\Delta\tau = 0.0001$. Employing the explicit finite difference scheme the above problem is simplified into the following set of finite difference equations:

$$\frac{\bar{U}_j - U_j}{\Delta\tau} - S\frac{U_j - U_{j-1}}{\Delta Y} = (1+\Delta)\frac{U_{j+1} - 2U_j + U_{j-1}}{(\Delta Y)^2} + \Delta\frac{\Omega_j - \Omega_{j-1}}{\Delta Y} + T_j \qquad \text{Eq. (13)}$$

$$\frac{\bar{\Omega}_j - \Omega_j}{\Delta\tau} - S\frac{\Omega_j - \Omega_{j-1}}{\Delta Y} = (1+.5\Delta)\left(\frac{\Omega_{j+1} - 2\Omega_j + \Omega_{j-1}}{(\Delta Y)^2}\right) - \Delta\Theta\left(2\Omega_j + \frac{U_j - U_{j-1}}{\Delta Y}\right) \qquad \text{Eq. (14)}$$

$$\frac{\bar{T}_j - T_j}{\Delta\tau} - S\frac{T_j - T_{j-1}}{\Delta Y} = \frac{1}{P_r}\left(\frac{T_{j+1} - 2T_j + T_{j-1}}{(\Delta Y)^2}\right) + (1+\Delta)E_C\left(\frac{U_j - U_{j-1}}{\Delta Y}\right)^2 \qquad \text{Eq. (15)}$$

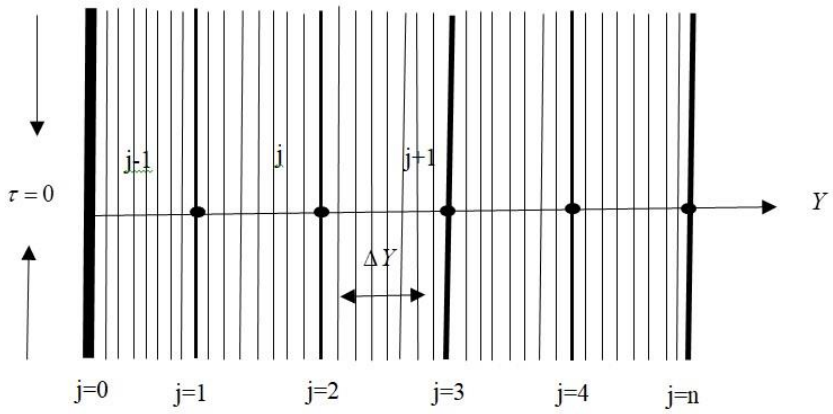

Figure 2. *Illustration of finite difference grid system.*

The boundary conditions, as defined by the finite difference method, are outlined as follows:

$$U_L = 0,\ \Omega_L = -N\frac{\partial U}{\partial Y},\ T_L = 1 \quad \text{at } Y = 1$$
$$U_L = \Omega_L = 0,\quad T_L = \varsigma \qquad \text{at } Y = -1 \qquad \text{Eq. (16)}$$

Shear stress, couple stress and nusselt number

The primary focus of this research has been represented by shear stress, couple stress and Nusselt number. The outcome of several parameters along shear stress at both the lower and upper planes derived from the velocity field. The local shear stress for the lower plate is $\tau_{L1} = \left[\mu + (1-n)\lambda\right]\left(\frac{\partial U}{\partial Y}\right)_{Y=-1}$ and for upper plate is $\tau_{L2} = \left[\mu + (1-n)\lambda\right]\left(\frac{\partial U}{\partial Y}\right)_{Y=1}$. The influence of relevant parameters on couple stress has been explored through analysis of the angular velocity field. The local couple Stress for the lower plate is $M_{L1} = \left(\frac{1}{1+\frac{\lambda}{2\mu}}\right)\left(\frac{\partial \Omega}{\partial Y}\right)_{Y=-1}$ and for upper plate is $M_{L2} = \left(\frac{1}{1+\frac{\lambda}{2\mu}}\right)\left(\frac{\partial \Omega}{\partial Y}\right)_{Y=1}$. The influence of relevant parameters on the Nusselt number has been assessed by analyzing the temperature distribution also. The local Nusselt number in the x-direction for the lower plate is denoted by $Nu_{L1} = \mu\left(-\frac{\partial T}{\partial Y}\right)_{Y=-1}$ while for the upper plate is represented as $Nu_{L2} = \mu\left(-\frac{\partial T}{\partial Y}\right)_{Y=1}$.

Stability and convergence criteria

The stability and the limit of convergence for the finite difference scheme have been investigated to ascertain the restrictions imposed by different relevant parameters. The whole procedure remains incomplete without stability and convergence analysis because the explicit procedure has been executed. After conducting a comprehensive stability analysis, the ultimate stability condition of the problem is expressed as follows:

$$\left(2\left(1+\Delta\right)\frac{\Delta\tau}{\left(\Delta Y\right)^2} - S\frac{\Delta\tau}{\Delta Y}\right) \le 1$$

$$\left(\left(1+.5\Delta\right)\frac{2\Delta\tau}{\left(\Delta Y\right)^2}-S\frac{\Delta\tau}{\Delta Y}+\Delta\Theta\Delta\tau\right)\le 1$$
$$\left(\left(\frac{1}{P_r}\right)\frac{2\Delta\tau}{\left(\Delta Y\right)^2}-S\frac{\Delta\tau}{\Delta Y}\right)\le 1 \qquad \text{Eq. (17)}$$

Where, taking $\Delta Y = 0.05,\ \Delta\tau = 0.0001$ and the starting condition, the convergence criteria of the model from the above equations are $0.04 \le P_r,\ \Delta \le 24,\ 500 \le S$ and $\Theta \le 400$.

Results and Discussion

To grasp the concept of the underlying physical phenomena of the aformentioned model, numerical computations were performed to attain values for the dimensionless velocity (υ), angular velocity (ω) and temperature (τ) under steady-state conditions. The influence of the Microrotation parameter (Δ), Suction parameter (s) in the presence of Prandtl number (P_r), Material parameter (Θ) Ratio parameter (ς), Eckert number (E_c) on the velocity (υ), angular velocity (ω) and temperature (τ) distributions are speculated through graphical representations. Furthermore the corresponding parameters shear stress, couple stress and Nusselt numbers has been discussed.

Justifying grid space

A mesh sensitivity analysis has been conducted as a part of this research. The calculations have been performed for obtaining the eligible mesh size for three different grid spacing (*m*,*n*)=(40,40); (*m*,*n*)=(60,60) and (*m*,*n*)=(80,80)are displayed in *Figure 3* where $E_C = .001;\ P_r = 7;\ \Delta = 4;\ \varsigma = .1;\ S = 0.5 \text{and}\ \Theta = 8.$. In this way, (*m*,*n*)=(40,40) has been selected as a suitable mesh size for the outcomes of the velocity, angular velocity and temperature fields, shear stress, couple stress and Nusselt number distribution.

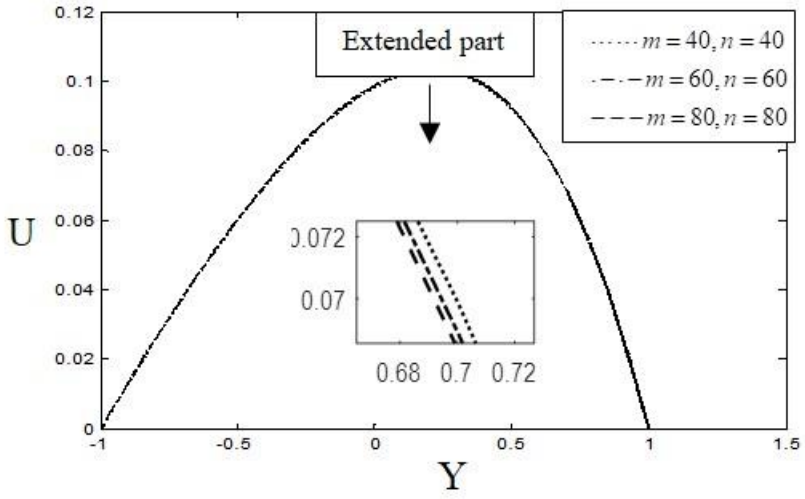

Figure 3. *The justifying grid space.*

Steady state solutions

Steady-state analysis has been performed on the formulated mathematical representation. The process was computed using six distinct dimensionless time interval durations like r=1.00, 2.00, 3.00, 6.00, 8.00 and 100 where $P_r = 7; E_c = .001; \Delta = 4; \varsigma = .1; S = 0.5$ and $\Theta = 8$ for obtaining time-sensitivity test. The outcome displays that little changes after and shows negligible changes up to r=3.00. *Figures 4* shows the steady-state solutions for velocity (U), angular velocity (Ω) and temperature (T).

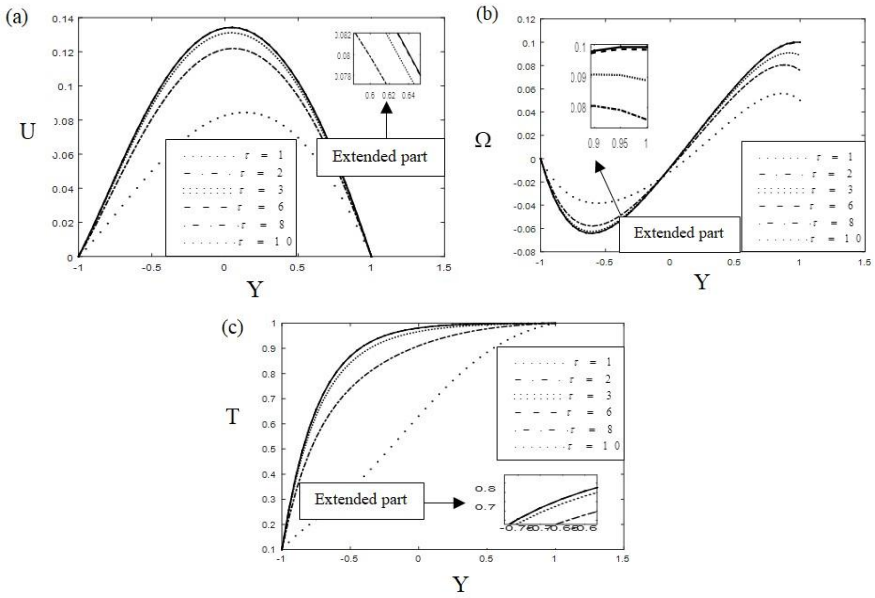

Figure 4. *The steady-state solutions for (a) velocity (U), (b) angular velocity (Ω) and (c) temperature (T).*

Effect of relevant parameters

For obtaining a comprehensive understanding of physical characteristics of this research, the impact of two parameters such as Microrotation parameter (Δ), Suction parameter (S) in the presence of Prandtl number (P_r), Material parameter (Θ), Ratio parameter (ς), Eckert number (E_c) on the velocity (U), angular velocity (Ω), and temperature profiles are visually displayed through *Figures 5* and *Figure 6*.

The Suction parameter (S) impact on velocity, angular velocity and temperature distribution has been presented in *Figure 5*. It has been seen from *Figure 5* that the velocity, angular velocity and temperature distribution has a minor increasing effect with the increase of the Suction parameter (S). Conversely, from *Figure 6* it can be discerned that the velocity, angular velocity and temperature distribution decrease as the Microrotation parameter (Δ) is increased. The effect of the Suction parameter (S) and Microrotation parameter (Δ) on velocity, angular velocity, temperature, local shear stress, couple stress and Nusselt number have illustrated in *Figures 7* to *Figure 10*. The observations from this figure reveal that velocity and temperature profile exhibit a decrease with the enhancement of the Microrotation parameter (Δ) and the Suction parameter (S) at both lower and upper plates. The angular velocity increases at the lower plate while it decreases at the upper plate with the increase of the Microrotation parameter (Δ) and the Suction parameter (S) both. On the lower plate, the local shear stress diminish with an increasing effect in the Microrotation parameter (Δ) and Suction parameter (S) both while at lower plate it increases with an increase in both parameters.

The couple stress experience an increases with the augmentation of both the Microrotation parameter (Δ) and the Suction parameter (S) at both lower and upper plates. Regarding the local Nusselt number at the lower plate it witness an increases with the increment of the Microrotation parameter (Δ) and the Suction parameter (S). Conversely, at the upper palte it decreases as both of the Microrotation parameter (Δ) and the Suction parameter (S) increase.

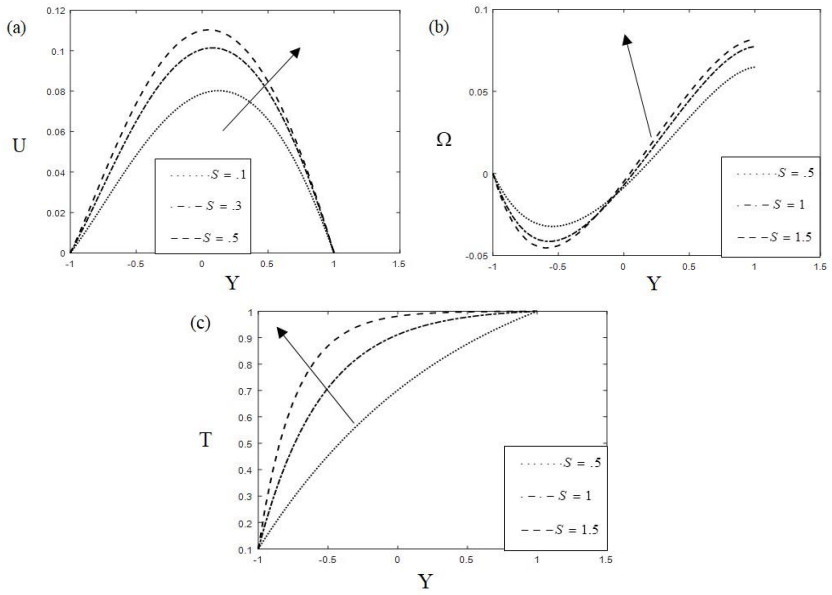

Figure 5. *Impact of non-dimensional Suction parameter (S) on (a) velocity, (b) angular velocity and (c) temperature profile; where $E_c = .001; \Delta = 5; P_r = 7; \varsigma = .1$ at time $\tau = 8(\text{steadystate})$.*

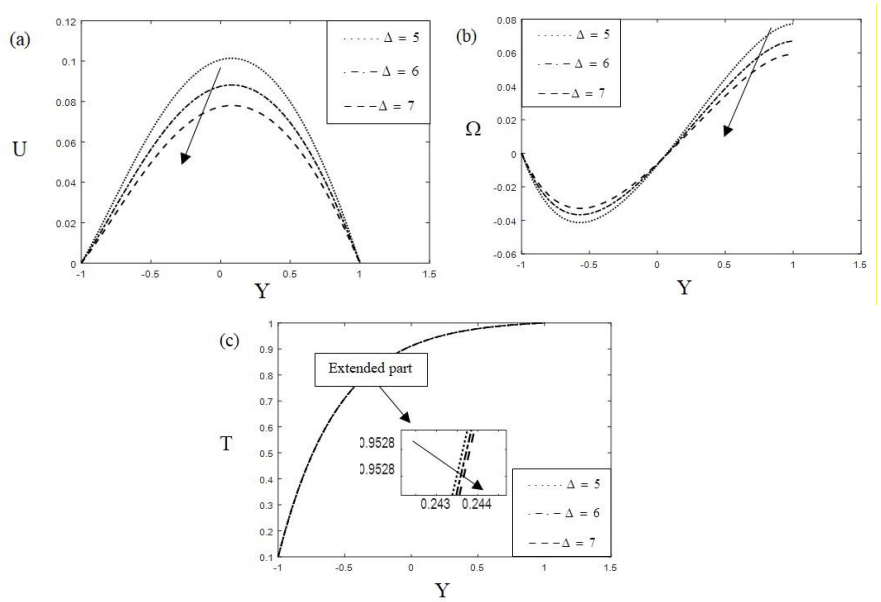

Figure 6. *Effects of dimensionless Microrotation parameter (Δ) on (a) velocity, (b) angular velocity and (c) temperature profile; where $E_c = .001; P_r = 7; \varsigma = 1$ and $S = .3$ at time $\tau = 8(\text{steadystate})$.*

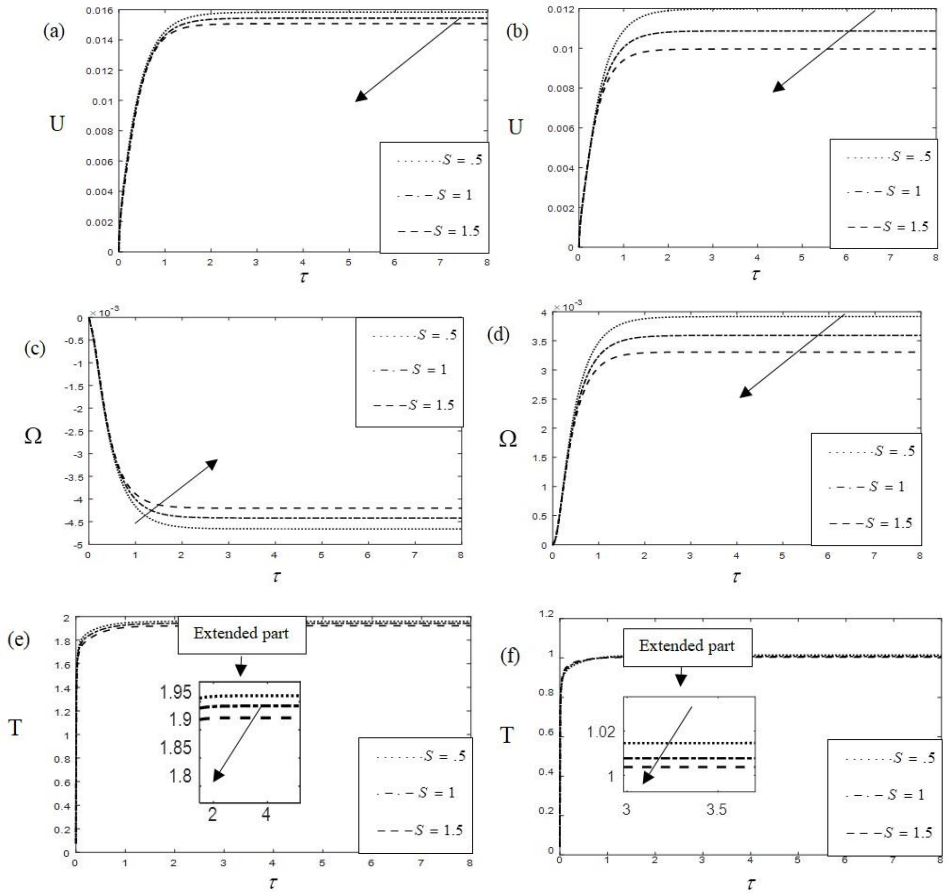

Figure 7. *Impact of non-dimensionl Suction parameter* (s) *on (a,b) velocity, (c,d) angular velocity and (e,f) temperature at both lower and upper plates; where* $E_c = .001; P_r = 1; \Theta = .8; \varsigma = 2 \text{and } \Delta = 4$ *at time* $\tau = 8(\text{steady state})$.

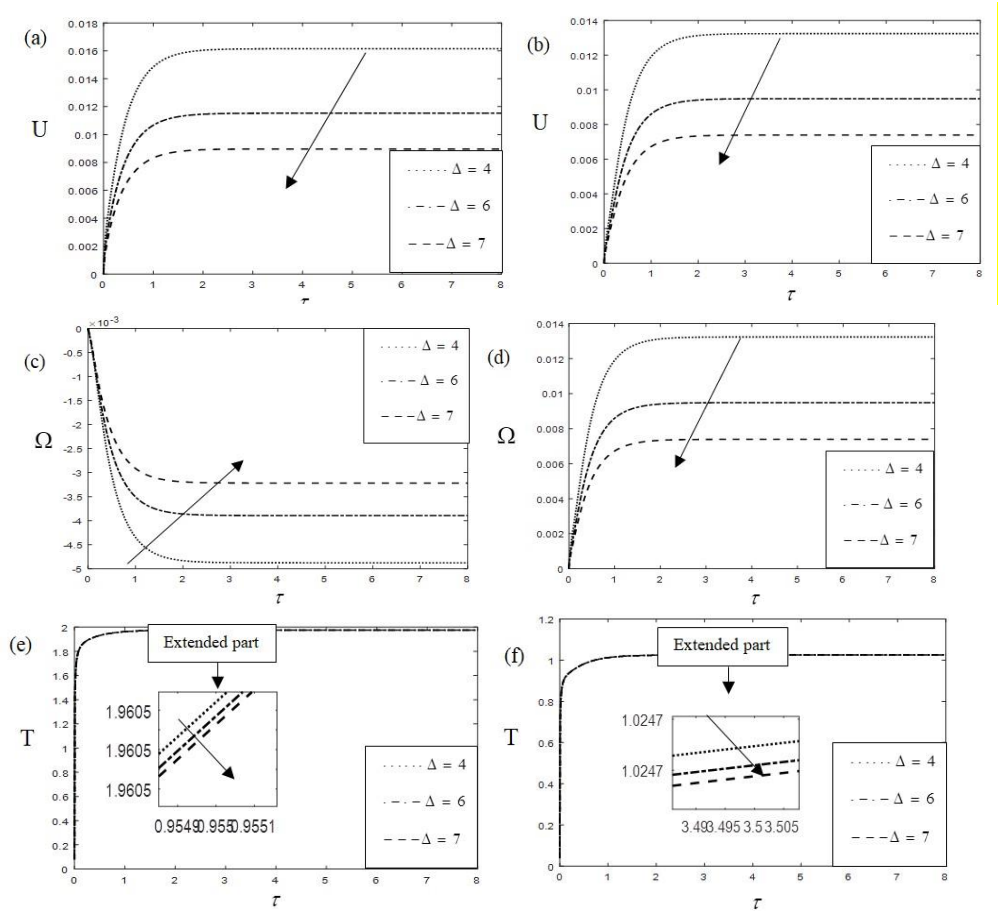

Figure 8. *Effects of dimensionless Microrotation parameter* (Δ) *on (a,b) velocity, (c,d) angular velocity and (e,f) temperature at both lower and upper plates; where* $E_C = .001; P_r = 1; \Theta = 4; \varsigma = 2$ and $S = .01$ *at time* $\tau = 8$(steady state).

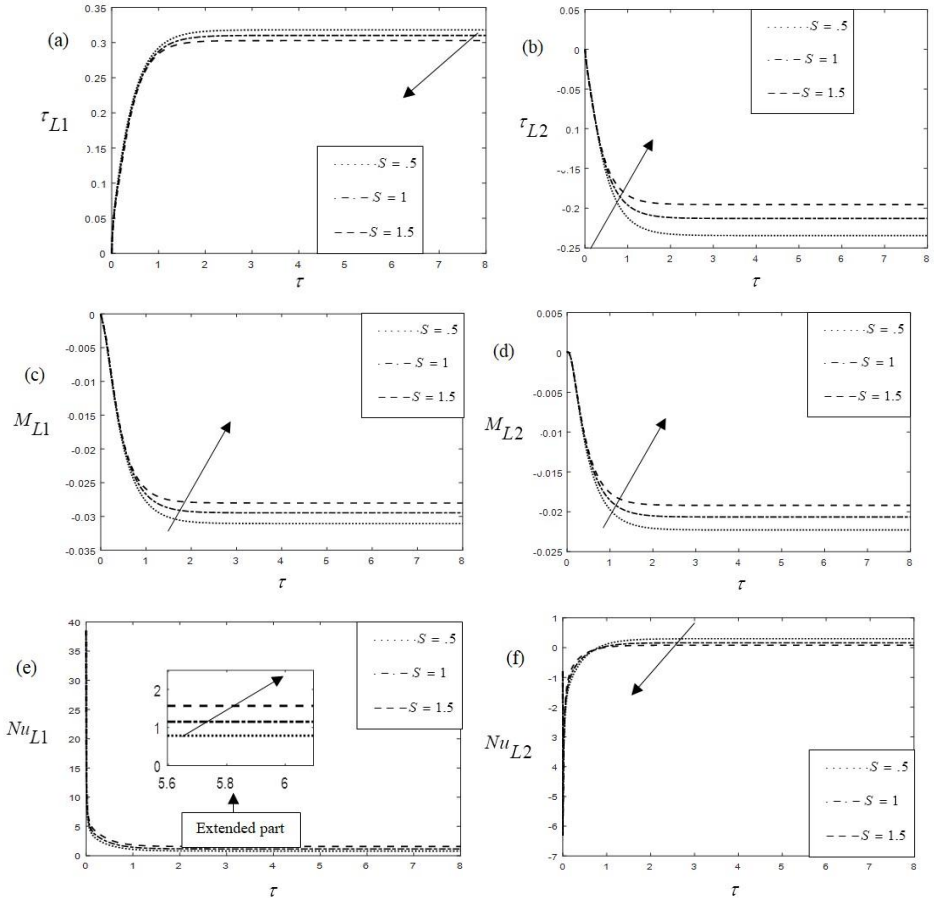

Figure 9. *Effects of dimensionless Suction parameter* $^{(S)}$ *on (a,b) local Shear stress, (c,d) local Couple stress and (e,f) local Nusselt number at both lower and upper plates; where* $E_C = .001; P_r = 1; \Theta = .8; \varsigma = 2 \text{and } \Delta = 4$ *at time* $\tau = 8(\text{steady state})$.

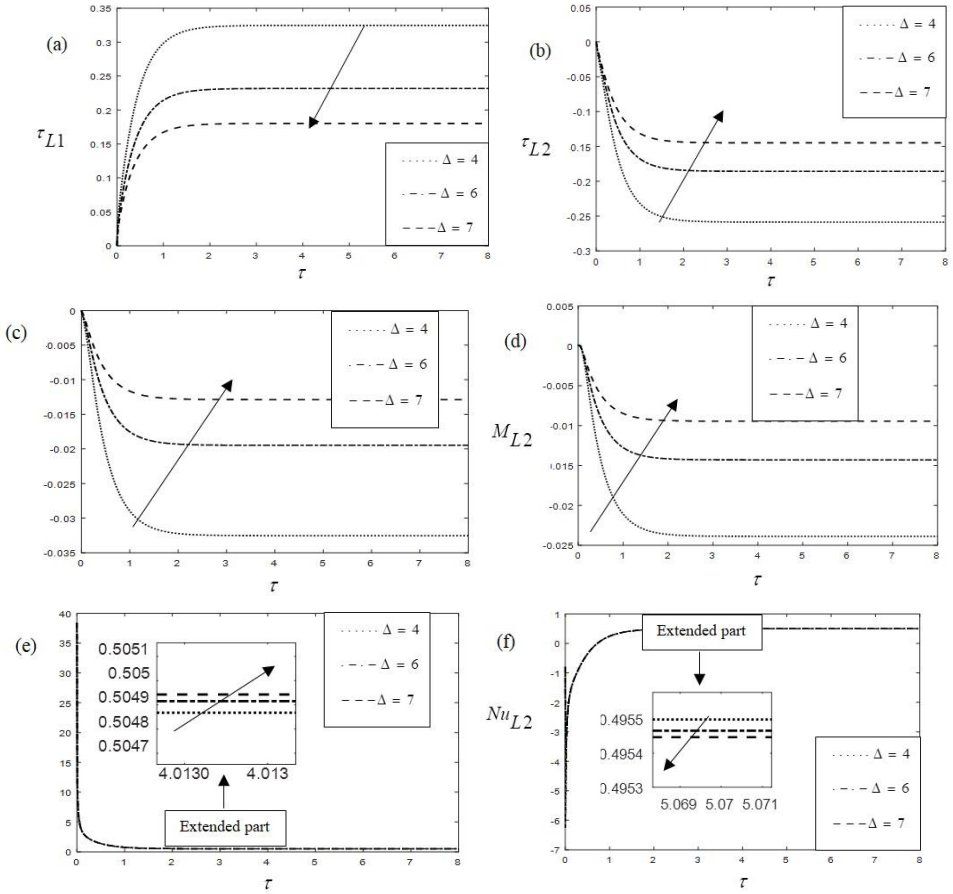

Figure 10. *Effects of dimensionless Microrotation parameter* (Δ) *on (a,b) local Shear stress, (c,d) local Couple stress and (e,f) local Nusselt number at both lower and upper plates; where* $E_c = .001; P_r = 1; \Theta = 4;\ \varsigma = 2$ and $S = .01$ *at time* $\tau = 8(\text{steadystate})$

Comparison

The validation for the finite difference scheme was computed by MATLAB R2015a for dimensionless velocity and a comparative analysis was made with the solutions obtained by studio Developer Fortran 6.6a. The outcomes from both tools are excellently agreed and demonstrating a strong consistency between the two method. The findings are same and consistent obtained through the mentioned tools. The simulations have been shown in *Figure 11* for distinct values of the Material parameter (Θ) on the velocity profile at the upper plate. *Figure 12* describes both a qualitative and quantitative comparison between the results of our outlines and those published by Bhargava et al. (2003); where $E_c = .001;\ P_r = .733; S = .5$ and $\Theta = .001.$ This comparisons aims to highlights similarities and difference between the two sets of findings for a comprehensive understanding of the research outcomes.

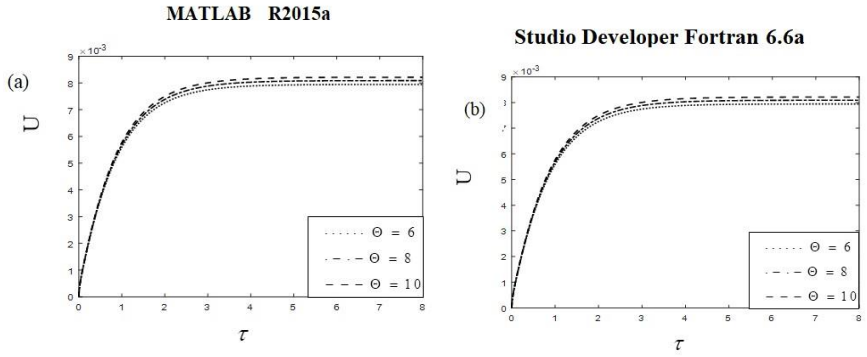

Figure 11. *Effects of dimensionless Material parameter* (Θ) *on (a,b) upon the velocity profile at upper plates.*

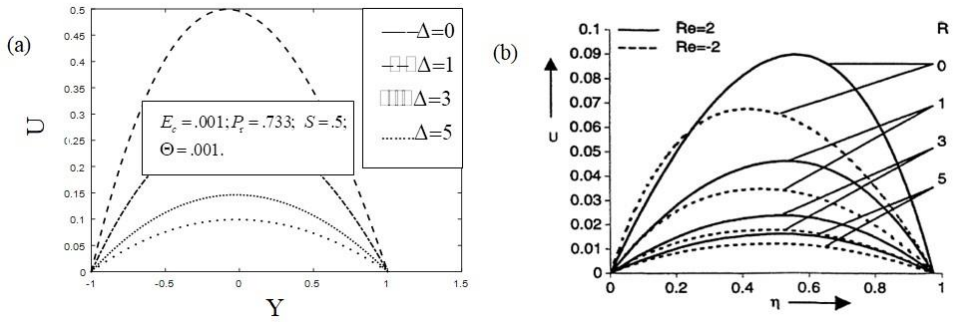

Figure 12. *Comparison of Microrotation parameter* (Δ) *on (a,b) upon the velocity profile with the published results of Bhargava et al. (2003); where* $E_c = .001;\ P_r = .733;\ S = .5$ and $\Theta = .001$.

Conclusion

The study investigated the numerical exploration of flow with unsteady natural convection within a micro-polar fluid confined amidst two horizontal parallel plates using the finite difference technique. To obtain steady-state solution, mesh sensitivity and time sensitivity analysis has been assessed to guarantee the precision and reliability of the numerical simulations in this research. The outcome is discussed for different relevant factors, including the Suction parameter and the Microrotation parameter and their flow pattern and behaviour were scrutinized. The most noteworthy outcomes of these studies are given as follows: (1) the velocity, angular velocity and temperature profile distribution is enhanced by (S); (2) The velocity, angular velocity and temperature profile distribution is reduced by (Δ); (3) the couple stress at both lower and upper plate enhanced with the increment of (S) and (Δ); (4) with the increment of (S) and (Δ) at both lower and upper plates, the velocity and temperature profile reduces; (5) with elevated values of (S) and (Δ), the angular velocity rises at the upper plate while it declines at lower plate; (6) with the increase of (S) and (Δ) both, the shear stress at the lower plate decreases and at the upper plate increases; and (7) The Nusselt number at the lower wall increases and at the upper wall reduces with the enhancement of (S) and (Δ) both.

Acknowledgement

This research is self-funded.

Conflict of interest

The authors confirm that there is no conflict of interest involve with any parties in this research study.

REFERENCES

[1] Bhargava, R., Kumar, L., Takhar, H.S. (2003): Numerical solution of free convection MHD micropolar fluid flow between two parallel porous vertical plates. – International Journal of Engineering Science 41(2): 123-136.
[2] Eringen, A.C. (1972): Theory of thermomicrofluids. – Journal of Mathematical Analysis and Applications 38(2): 480-496.
[3] Eringen, A.C. (1966): Theory of micropolar fluids. – Journal of mathematics and Mechanics 18p.
[4] Eringen, A.C. (1964): Simple microfluids. – International Journal of Engineering Science 2(2): 205-217.
[5] Galdi, G.P., Rionero, S. (1977): A note on the existence and uniqueness of solutions of the micropolar fluid equations. – International Journal of Engineering Science 15(2): 105-108.
[6] Hayat, T., Sajjad, R., Ellahi, R., Alsaedi, A., Muhammad, T. (2017): Homogeneous-heterogeneous reactions in MHD flow of micropolar fluid by a curved stretching surface. – Journal of Molecular Liquids 240: 209-220.
[7] Lok, Y.Y., Pop, I., Ingham, D.B. (2010): Oblique stagnation slip flow of a micropolar fluid. – Meccanica 45: 187-198.
[8] Mohanty, B., Mishra, S.R., Pattanayak, H.B. (2015): Numerical investigation on heat and mass transfer effect of micropolar fluid over a stretching sheet through porous media. – Alexandria Engineering Journal 54(2): 223-232.
[9] Mujaković, N. (2010): One-dimensional compressible viscous micropolar fluid model: stabilization of the solution for the Cauchy problem. – Boundary Value Problems 21p.
[10] Mujaković, N. (1998): One-dimensional flow of a compressible viscous micropolar fluid: a global existence theorem. – Glasnik Matematički 33(2): 199-208.
[11] Patel, H.R. (2021): Thermal radiation effects on MHD flow with heat and mass transfer of micropolar fluid between two vertical walls. – International Journal of Ambient Energy 42(11): 1281-1296.
[12] Rahman, M.M., Sattar, M.A. (2007): Transient convective flow of micropolar fluid past a continuously moving vertical porous plate in the presence of radiation. – Applied Mechanics and Engineering 12(2): 497-513.
[13] Ravi, S.K., Singh, A.K., Singh, R.K., Chamkha, A.J. (2013): Transient free convective flow of a micropolar fluid between two vertical walls. – International Journal of Industrial Mathematics 5(2): 87-95.
[14] Takhar, H.S., Soundalgekar, V.M. (1985): Flow and heat transfer of micropolar fluid past a porous plate. – Indian Journal of Pure and Applied Mathematics 16(5): 552-558.
[15] Turkyilmazoglu, M. (2016): Flow of a micropolar fluid due to a porous stretching sheet and heat transfer. – International Journal of Non-Linear Mechanics 83: 59-64.